Optimal path of diffusion over the saddle point and fusion of massive nuclei

Chun-Yang Wang,[1] Ying Jia,[2] and Jing-Dong Bao[1,3,*]

[1]*Department of Physics, Beijing Normal University, Beijing 100875, People's Republic of China*

[2]*College of Science, The Central University for Nationalities, Beijing 100081, People's Republic of China*

[3]*Center of Theoretical Nuclear Physics, National Laboratory of Heavy-ion Accelerator, Lanzhou 730000, People's Republic of China*

(Received 23 May 2007; published 11 February 2008)

The diffusion of a particle passing over the saddle point of a two-dimensional quadratic potential is studied via a set of coupled Langevin equations, and the expression for the passing probability is obtained exactly. The passing probability is found to be strongly influenced by the off-diagonal components of inertia and friction tensors. If the system undergoes the optimal path to pass over the saddle point by taking an appropriate direction of initial velocity into account, which departs from the potential valley and has minimum dissipation, the passing probability should be enhanced. Applying this to the fusion of massive nuclei, we show that there exists an optimal injection choice for the deformable target and projectile nuclei, namely, the intermediate deformation between spherical and extremely deformed nuclei, that maximizes the fusion probability.

DOI: 10.1103/PhysRevC.77.024603 PACS number(s): 24.10.−i, 24.60.−k, 25.70.Jj, 05.20.−y

I. INTRODUCTION

The saddle-point passage problem is of great interest in various fields of physics, such as those involving collisions of molecular systems, atomic clusters, and biomolecules. Previous studies on this issue mostly concentrated on simple diffusive dynamics with a single degree of freedom, where the Langevin equation with constant coefficients can be easily solved in the case of a quadratic potential [1]. However, because many processes obviously involve more than one degree of freedom, for which the one-dimensional (1D) model does not distinctly hold, dimensions of higher degree are necessary. A case in point would be the fusion reaction of massive nuclei, where the fusion is induced by diffusion [2,3] and the asymmetrical or the neck degree of freedom of the compound nuclei needs to be considered [4,5]. For such systems where the contact point of two colliding nuclei are very close to the conditional saddle point, the potential energy surface (PES) around the saddle point can be approximated to be a quadratic type. Under this approximation, Abe *et al*. [6] obtained an analytical expression for the multidimensional saddle-point passing probability. Some authors discussed the quantum effect of the fusion probability by using the real-time path integral [7] or the quantum transport equation [8,9], respectively. Boilley *et al*. [10] studied the influence of initial distribution upon the passing probability. Anomalous diffusion passing over the saddle point of the 1D quadratic potential was also discussed in Ref. [11]. Nevertheless, the dynamical role of nontransport degrees of freedom is not completely clear. This might be very important for the quasi-fission mechanism in the fusion reaction, because the average path of the fusing system in a multidimensional PES should be controlled by the off-diagonal components of inertia and friction tensors before the system first arrives at the conditional saddle point.

Recently, theoretical calculations for the fusion barrier distribution, accounting for the surface curvature correction to the nuclear potential, have been presented by Hinde and co-workers [12–14]. The geometrical effect significantly changes the near-barrier fusion cross section and the shape of the barrier distribution through an angle-dependent potential, where the target nucleus bears quadrupole and bexadecapole deformations and the projectile is of spherical shape. In these calculations, the surface curvature correction to the sphere-to-sphere nuclear potential influences the fusion probability through the height of the fusion barrier. However, the dynamical coupling effect of various deformative degrees of freedom needs to be added from the viewpoint of fusion by diffusion [3].

The primary purpose of this paper is to study the influence of coupling between two degrees of freedom upon the passing probability. In Sec. II, we report the analytical expression of the saddle-point passing probability by solving the two-dimensional (2D) coupled Langevin equation with constant coefficients. In Sec. III, we discuss the effects of off-diagonal components of inertia, friction, and potential-curvature tensors and then determine the optimal diffusive path. Section IV gives an application of this study to the actual fusion process of massive nuclei. A summary is written in Sec. V.

II. THE PASSING PROBABILITY

We consider the directional diffusion of a particle in a 2D quadratic PES: $U(x_1, x_2) = \frac{1}{2}\omega_{ij}x_i x_j$ with $i, j = 1, 2$ and $\det \omega_{ij} < 0$. The motion of the particle is described by the Langevin equation

$$m_{ij}\ddot{x}_j(t) + \beta_{ij}\dot{x}_j(t) + \omega_{ij}x_j(t) = \xi_i(t), \tag{1}$$

with $x_j(0) = x_{j0}$ and $\dot{x}_j(0) = v_{j0}$, where $x_{10} < 0$ and $v_{10} > 0$. Here and in the following the Einstein summation convention is used. The two components of the random force are assumed to be Gaussian white noises and their correlations obey the fluctuation-dissipation theorem $\langle \xi_i(t)\xi_j(t')\rangle = k_B T m^{-1}_{ik}\beta_{kj}\delta(t - t')$, where k_B is the Boltzmann constant and T is the temperature.

*Corresponding author; electronic address: jdbao@bnu.edu.cn

Assuming that x_1 axis is the transport direction [$\omega_{11} < 0$], we write the reduced distribution function of the particle for x_1 while the variables $x_2(t)$, $v_1(t)$, and $v_2(t)$ are integrated out:

$$W(x_1, t; x_{10}, x_{20}, v_{10}, v_{20}) = \frac{1}{\sqrt{2\pi}\sigma_{x_1}(t)} \exp\left(-\frac{[x_1(t) - \langle x_1(t)\rangle]^2}{2\sigma_{x_1}^2(t)}\right). \quad (2)$$

Integrating over x_1 from zero to infinity, we determine the passing probability over the saddle point [$x_1 = x_2 = 0$] as

$$P(t; x_{10}, x_{20}, v_{10}, v_{20}) = \int_0^\infty W(x_1, t; x_{10}, x_{20}, v_{10}, v_{20})\, dx_1 = \frac{1}{2}\mathrm{erfc}\left(-\frac{\langle x_1(t)\rangle}{\sqrt{2}\sigma_{x_1}(t)}\right). \quad (3)$$

Applying the Laplace transform technique to Eq. (1), we thus get $x_1(t)$ and its variance $\sigma_{x_1}^2(t)$ at any time:

$$x_1(t) = \langle x_1(t)\rangle + \sum_{i=1}^{2} \int_0^t H_i(t - t')\xi_i(t')dt', \quad (4)$$

$$\sigma_{x_1}^2(t) = \int_0^t dt_1 H_i(t - t_1) \int_0^{t_1} dt_2 \langle \xi_i(t_1)\xi_j(t_2)\rangle H_j(t - t_2), \quad (5)$$

where the mean position of the particle along the transport direction is given by

$$\langle x_1(t)\rangle = \sum_{i=1}^{2} [C_i(t)x_{i0} + C_{i+2}(t)v_{i0}], \quad (6)$$

which relates to the initial position and velocity. The time-dependent factors in Eq. (6) with exponential forms according to the residual theorem are $C_i(t) = \mathcal{L}^{-1}[\mathrm{F}_i(s)/\mathrm{P}(s)]$ ($i = 1, \ldots, 4$), and the two response functions in Eqs. (4) and (5) read $\mathrm{H}_1(t) = \mathcal{L}^{-1}[\mathrm{F}_5(s)/\mathrm{P}(s)]$ and $\mathrm{H}_2(t) = \mathcal{L}^{-1}[\mathrm{F}_6(s)/\mathrm{P}(s)]$, where $\mathcal{L}^{-1}$ denotes the inverse Laplace transform. The expressions of $P(s)$ and $F_i(s)$ ($i = 1, \ldots, 6$) are given in the Appendix.

III. THE OPTIMAL DIFFUSIVE PATH

A. The coupling effect of two degrees of freedom

As is known in the 1D case, the passing probability increases from 0 to 1 when the initial velocity of the particle increases. The critical velocity is defined by the passing probability being equal to 1/2. This leads to the following condition: $\lim_{t\to\infty}\langle x_1(t)\rangle = 0$. If we ignore all the off-diagonal components of the three coefficient tensors, and take x_{20} and v_{20} to be zero, the critical velocity is determined from Eq. (6): $v_0^c = [\mathrm{F}_1(a)/\mathrm{F}_3(a)]x_{10}$, where a is the largest positive root of $\mathrm{P}(s) = 0$. This is in fact identical to the 1D result: $v_{10}^c = -x_{10}(\sqrt{\beta_{11}^2 + 4\omega_{11}} + \beta_{11})/(2m_{11})$ [6], which is proportional to the friction strength.

We now consider all the off-diagonal components of the three coefficient tensors; that is, we take the correlations of two degrees of freedom into account. The critical velocity can also be determined by $\lim_{t\to\infty}\langle x_1(t)\rangle = 0$, resulting in

$$v_0^c = -\frac{C_1(\infty)x_{10} + C_2(\infty)x_{20}}{C_3(\infty)\cos\theta + C_4(\infty)\sin\theta}, \quad (7)$$

where θ denotes the incident angle between the initial velocity and the x_1 direction; hence $v_{10} = v_0\cos\theta$ and $v_{20} = v_0\sin\theta$.

In Fig. 1, we plot the critical velocity and the stationary passing probability as functions of the off-diagonal components of the three coefficient tensors, where one of the off-diagonal components varies and the other two are fixed to be zero. Note that the quantities plotted in Figs. 1–7 are dimensionless and $k_B = 1.0$ except for the units having been included in the figure caption. The stationary passing probability is calculated by $P_{\mathrm{pass}} = \lim_{t\to\infty}\frac{1}{2}\mathrm{erfc}\{-\langle x_1(t)\rangle/[\sqrt{2}\sigma_{x_1}(t)]\}$. It is seen that the critical velocity increases with increasing absolute value of m_{12} or ω_{12} whereas it decreases with an increase of $|\beta_{12}|$. The larger the critical velocity a system needs, the more difficult it is for the particle to arrive at the top of the potential. This also implies that the passing probability is small when the dissipation along the diffusive path is large if the potential differences between the saddle point and the initial positions are equivalent. As is shown in the figure, the behavior of the passing probability is opposite to that of the corresponding critical velocity.

Figure 2 shows the stationary passing probability in the presence of two off-diagonal components ω_{12} and β_{12}, simultaneously, for $m_{12} = 0$. It is seen that the maximum of the passing probability does not appear in the vertical case ($\omega_{12} = 0$). In the 2D PES, the particle is usually supposed to travel along the potential valley and then the steepest decedent direction, because this is the direction that faces a smaller potential barrier. However, it may not be a path with a weaker damping. Under the effect of the off-diagonal component of the friction tensor, the particle is forced to select a better path with both low potential barrier and weak friction to surmount the saddle point of the potential.

B. Determination of the optimal path

Where is the optimal incident direction that enables the particle with given initial kinetic energy to have a larger passing probability? To determine this direction, we need to choose a special angle θ_m that enables the critical velocity to reach its minimum, that is, from Eq. (7),

$$\left.\frac{dv_0^c}{d\theta}\right|_{\theta=\theta_m} = 0, \quad \theta_m = \arctan\left(\frac{C_4(\infty)}{C_3(\infty)}\right). \quad (8)$$

In fact, the largest analytical root of $P(s) = 0$ dominantly determines the passing probability. The optimal incident angle θ_m can then be expressed by the Langevin coefficients as

$$\theta_m = \arctan\left(\frac{m_{12}(\beta_{22}a + \omega_{22}) - m_{22}(\beta_{12}a + \omega_{12})}{m_{11}F_5(a) + m_{12}F_6(a)}\right). \quad (9)$$

Using the same parameters as those written in Figs. 1 and 3, we obtain $\theta_m \simeq 0.258$ rad, as is explicitly shown in Fig. 3, corresponding to the maximum of the stationary passing probability.

We now define γ, ψ, and α to be the rotation angles of the major axis of the potential-curvature, friction, and inertia

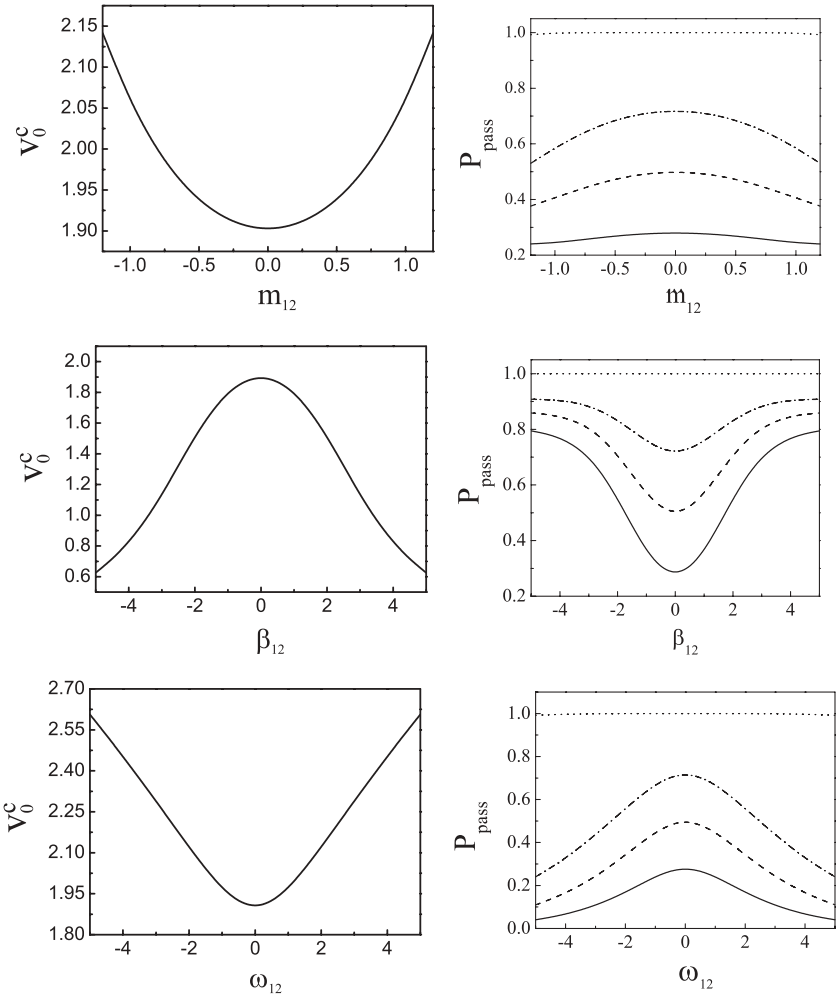

FIG. 1. The critical velocity (left) and the stationary passing probability (right) as functions of various off-diagonal components m_{12}, β_{12}, and ω_{12}, respectively. The parameters used are $m_{11} = 1.5$, $m_{22} = 2.0$, $\beta_{11} = 1.8$, $\beta_{22} = 1.2$, $\omega_{11} = -2.0$, $\omega_{22} = 1.5$, and $\theta = 0$. The initial velocities of the particle are $v_0 = 4.0$, 2.2, 1.9, and 1.6 from top to bottom (right).

tensors, respectively. They are found to have the following expressions:

$$\tan 2\gamma = \frac{2\omega_{12}}{\omega_{22} - \omega_{11}}, \quad \tan 2\psi = \frac{2\beta_{12}}{\beta_{22} - \beta_{11}}, \quad \tan 2\alpha = \frac{2m_{12}}{m_{22} - m_{11}}. \tag{10}$$

As an example, for the case we have studied in Figs. 1 and 3, these angles are $\gamma \simeq -7.973^\circ$, $\psi \simeq -34.722^\circ$, and $\alpha \simeq 33.690^\circ$. For comparison, the optimal incident direction of the particle we have obtained for the 2D calculation is $\theta_m \simeq 14.779^\circ$ (0.258 rad).

In Fig. 4, we plot the two-dimensional quadratic potential and the optimal path in the x_1-x_2 plane as a schematic illustration. All the coefficient elements used here have been

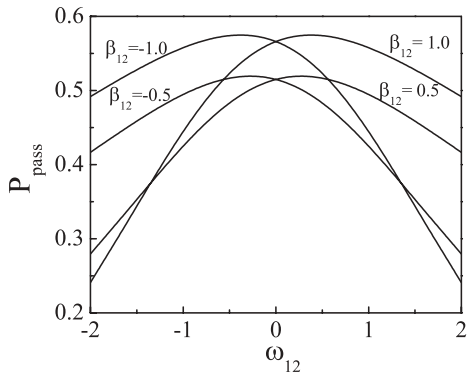

FIG. 2. The stationary passing probability as a function of the off-diagonal component ω_{12} for various β_{12} values. The parameters used are the same as those in Fig. 1.

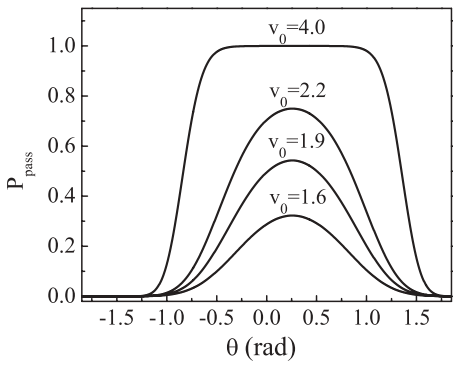

FIG. 3. The stationary passing probability as a function of the incident angle. Here $m_{12} = 0.6$, $\beta_{12} = 0.8$, and $\omega_{12} = -0.5$; the other parameters are the same as those in Fig. 1.

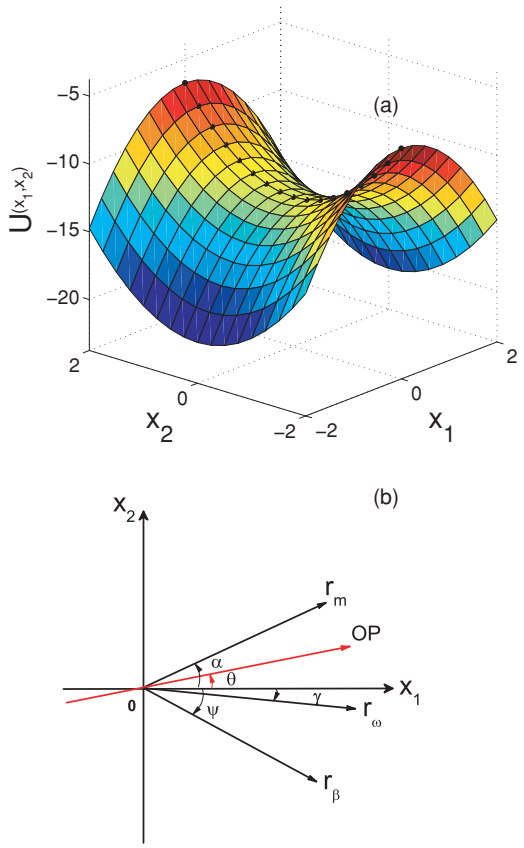

FIG. 4. (Color online) (a) The 2D potential energy surface, where the dotted curve is the saddle ridge line. (b) A schematic illustration of the optimal diffusion path (OP), where $\mathbf{r}_m$, $\mathbf{r}_\beta$, and $\mathbf{r}_\omega$ denote the major axes of the inertia, friction, and potential-curvature tensors, respectively.

written in Figs. 1 and 3. The figure illustrates that the direction of the optimal path departs from the x_1 direction. The effect of the off-diagonal component of the inertia tensor makes the average path of the diffusive system turn toward the positive x_2 axis, whereas the off-diagonal component of friction leads the mean path of the particle toward the negative x_2 axis. Finally, the competition of these two effects results in the optimal diffusive path shown in Fig. 4(b). This phenomenon is similar to the quasi-stationary flow passing over the barrier in the fission case [15], where the magnitude of the current is strongly influenced by the off-diagonal components of inertia and friction tensors.

Figure 5 shows the dependence of the stationary passing probability on the incident angle of the particle starting from various initial positions but with fixed initial kinetic energy. It is seen that the passing probability of the particle starting from a large positive x_{20} position is larger than that starting from both small and negative x_{20} positions. This difference occurs because the energy difference between the top of the potential and the initial position of the particle is small for the former. Amusingly, we find that the difference between the passing probabilities of two symmetrical positions $(-1.0, -0.5)$ and $(-1.0, 0.5)$ is observably large.

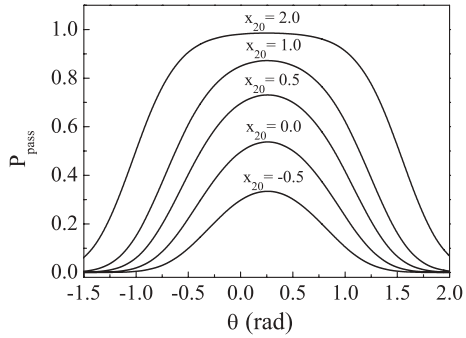

FIG. 5. The stationary passing probability as a function of θ for various x_{20} values. Here $x_{10} = -1.0$, $v_0 = 1.9$, $m_{12} = 0.6$, $\beta_{12} = 0.8$, and $\omega_{12} = -0.5$; the other parameters are the same as in Fig. 1.

For a clearer understanding of these results, we plot in Fig. 6 the mean diffusive path of a particle starting from different initial positions with different incident angles. Here $\langle x_1(t)\rangle$ has been obtained in Eq. (6) and

$$\langle x_2(t)\rangle = \sum_{i=1}^{2} [C_{i+4}(t)x_{i0} + C_{i+6}(t)v_{i0}], \qquad (11)$$

where all the time-dependent quantities are given in the Appendix. The critical velocities are calculated by using Eq. (7): $v_0^c = 1.5791$ when $x_{20} = 0.5$; $v_0^c = 2.2321$ when $x_{20} = -0.5$, for $x_{10} = -1.0$ and $\theta = 0$. Hence the stationary passing probability of the particle starting from $x_{20} = 0.5$ is larger than that of the particle starting from $x_{20} = -0.5$. In particular, under the present circumstance, the diffusive process of a particle with different incident angles shows an interesting behavior. Because the initial velocity of the particle along the x_1 direction for $\theta = 0$ is larger than that for $\theta = 0.258$ rad, the former can move to a position being

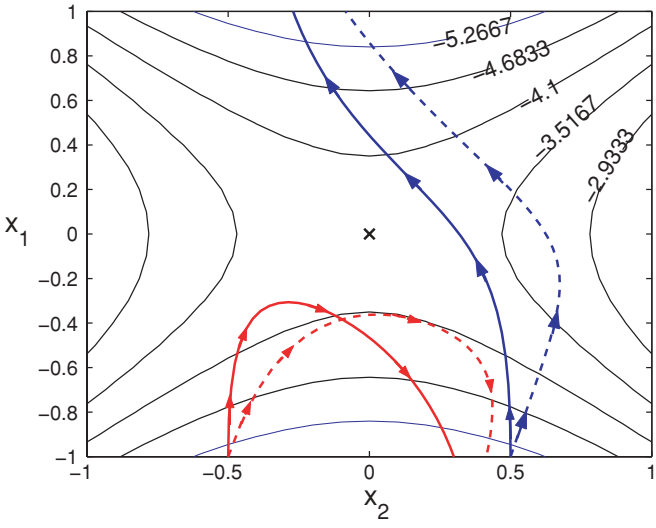

FIG. 6. (Color online) The mean diffusion path of a particle starting from two different initial positions at fixed $v_0 = 1.9$, where the solid and dashed lines correspond to $\theta = 0$ rad and $\theta = 0.258$ rad, respectively. Here all the Langevin parameters are the same as in Figs. 1 and 5.

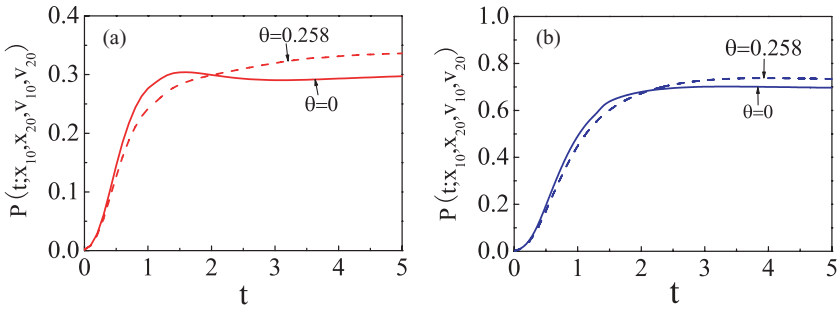

FIG. 7. (Color online) Time-dependent passing probability for various x_{20} and θ. Here $x_{10} = -1.0$, $v_0 = 1.9$, and (a) $x_{20} = -0.5$ and (b) $x_{20} = 0.5$; the Langevin parameters are the same as in Figs. 1 and 5.

closer to the saddle point than the latter. Thus the passing probability for $\theta = 0$ is larger than that of $\theta = 0.258$ rad at the beginning. However, the width of the Gaussian distribution is independent of the incident angle and increases with time. Although the center position of the particle's distribution with $\theta = 0.258$ rad is behind that of $\theta = 0$, as time goes on, it will have a lager share of its distribution past the saddle point. Therefore, the passing probability for a particle with incident angle $\theta = 0.258$ rad is larger than that with $\theta = 0$ for long times.

The time-dependent passing probabilities shown in Figs. 7(a) and 7(b) are also in complete agreement with this theoretical analysis.

IV. APPLICATION TO FUSION OF MASSIVE NUCLEI

We now apply the present 2D simplified diffusive model to investigate the fusion of two massive nuclei, which has been described by directional diffusion over the saddle point [6]. As a particular example, we calculate the fusion probability of the nearly symmetrical reaction system ^{100}Mo + ^{110}Pd [16], which is plotted as a function of the center-of-mass energy $E_{\text{c.m.}}$ in Fig. 8. A schematic illustration of the deformation of the compound nucleus is also shown in this figure. The temperature of the fusing system is determined by $aT^2 = E_{\text{c.m.}} + Q - E_B$, where $a = A/10$ is the energy level constant with A the nucleon number of the compound nucleus, Q denotes the reaction Q value, and E_B is the barrier height of the fission potential.

The $\{c, h, \alpha\}$ shape parametrization [17] with elongation c (half the nuclear length) and neck variable h are used (i.e., $x_1 = c, x_2 = h$), and the asymmetrical parameter α is fixed to be zero. The inertia and friction tensors are calculated by the Werner-Wheeler method and the one-body dissipative mechanism [18], respectively; all the Langevin coefficients are considered to be constants at the saddle point. The three components of the potential-curvature tensor are $\omega_{11} = -28.2304$, $\omega_{22} = 275.4211$, and $\omega_{12} = 50.4551$ in units of MeV; the components of friction tensor are $\beta_{11} = 701.9967$, $\beta_{22} = 621.4425$, and $\beta_{12} = 601.4934$ in units of 10^{-21} MeV $\cdot$ s; the inertia elements are $m_{11} = 102.4081$, $m_{22} = 134.4673$, and $m_{12} = 110.3783$ in units of 10^{-42} MeV $\cdot$ s^2.

We highlight an interesting result from Fig. 8: There exists an optimal collision shape for projectile and target nuclei that induces the maximum fusion probability under the same center-of-mass energy. This can be easily understood from the combining role of the off-diagonal components of the three dynamical coefficient tensors. Thus the fusion probability of massive nuclei can be enhanced if the two collision heavy ions are polarized to be ellipsoidal and the collision direction between the long and short axes of the ellipsoid is appropriately selected. For the fusion of deformed massive nuclei, there exists an optimal angle for the incident nucleus to collide with the target one, which favors the fusion of heavy ions.

Figure 9 shows the fusion probability of ^{100}Mo + ^{110}Pd as a function of the center-of-mass energy when the off-diagonal components are partly considered. Here the initial position

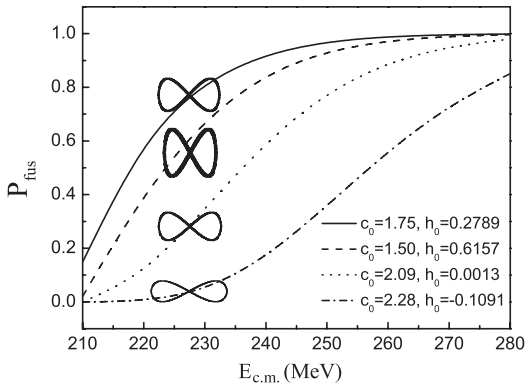

FIG. 8. The fusion probability of the reaction ^{100}Mo + ^{110}Pd as a function of the center-of-mass energy for various initial positions. Schematically illustrated as well are the deformed shapes of the compound nucleus.

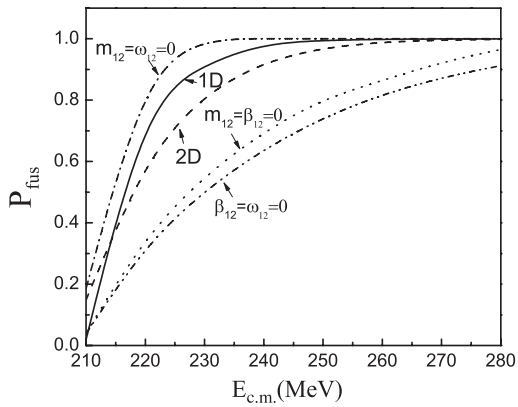

FIG. 9. The fusion probability of the reaction ^{100}Mo + ^{110}Pd as a function of the center-of-mass energy for the situations with and without off-diagonal components.

of the fusing system is chosen as the optimal one (i.e., $c_0 = 1.75$ and $h_0 = 0.2789$) and the parameters used are the same as in Fig. 8. This fusion reaction system serves as an example with which to compare the results with and without off-diagonal components in the potential surface, friction, and mass parameters, which is reflected in the result presented earlier. In fact, the case without any off-diagonal components is equivalent to the the one-dimensional case or the case without the neck variable [4].

It is seen from Fig. 9 that the increase of the 1D fusion probability curve versus energy is greater than that of the 2D case. It has been known that the previous 1D diffusion model without the neck variable gave a fusion probability larger than that found from the experimental data, so the present, completely coupled, 2D diffusion model might be appropriate. Moreover, the results for the presence of only one of three off-diagonal components can also be understood from the critical velocity (kinetic energy; see Fig. 1). Namely, the larger the critical kinetic energy of the system is, the less the fusion probability is for the same center-of-mass energy. The nonvanishing β_{12} allows the smallest critical kinetic energy and the presence of m_{12} leads to the largest critical kinetic energy. Therefore, we have a relation for the fusion probabilities: $P_{\rm fus}(\beta_{12} \neq 0) > P_{\rm fus}(\omega_{12} \neq 0) > P_{\rm fus}(m_{12} \neq 0)$ at a fixed center-of-mass energy.

V. SUMMARY

We have studied the diffusion process of a particle passing over the saddle point of a two-dimensional nonorthogonal quadratic potential. The expression of the passing probability is obtained analytically, where the inertia and friction tensors are not diagonal. The optimal incident angle of the particle's initial velocity is determined. Our results have shown that the optimal diffusive path, which departs from the potential valley in the two-dimensional potential energy surface, induces the maximum saddle-point passing probability. This is due to the competition among the off-diagonal components of inertia, friction, and potential-curvature tensors. We have investigated the fusion probability of massive nuclei and compared the results with and without off-diagonal terms, for instance, for the reaction of ^{100}Mo + ^{110}Pd. Because of the influences of off-diagonal components of inertia and friction upon the diffusive path, which are calculated by the $\{c, h, \alpha\}$ parametrization, the fusion probability can be enhanced for an appropriate choice of the collision direction of the deformable target and projectile nuclei. The optimal configuration of colliding nuclei is between spherical and extremely deformed ones. The present study also provides useful information in connection with the synthesis of superheavy elements.

ACKNOWLEDGMENTS

This work was supported by the National Natural Science Foundation of China under Grant Nos. 10674016 and 10747166 and by the Specialized Research Foundation for the Doctoral Program of Higher Education under Grant No. 20050027001.

APPENDIX: THE EXPRESSIONS OF $\langle x_1(t)\rangle$ AND $\langle x_2(t)\rangle$

The quantities appearing in the expression of $\langle x_1(t)\rangle$ are

$$\begin{aligned}
\mathrm{P}(s) &= (\det m)s^4 + (m_{11}\beta_{22} + m_{22}\beta_{11} - 2m_{12}\beta_{12})s^3 \\
&\quad + (\det\beta + m_{11}\omega_{22} + m_{22}\omega_{11} - 2m_{12}\omega_{12})s^2 \\
&\quad + (\beta_{11}\omega_{22} + \beta_{22}\omega_{11} - 2\beta_{12}\omega_{12})s + \det\omega, \\
\mathrm{F}_1(s) &= (\det m)s^3 + (m_{11}\beta_{22} + m_{22}\beta_{11} - 2m_{12}\beta_{12})s^2 \\
&\quad + (\det\beta + m_{11}\omega_{22} - m_{12}\omega_{12})s + \beta_{11}\omega_{22} - \beta_{12}\omega_{12}, \\
\mathrm{F}_2(s) &= (m_{12}\omega_{22} - m_{22}\omega_{12})s + \beta_{12}\omega_{22} - \beta_{22}\omega_{12}, \qquad \text{(A1)} \\
\mathrm{F}_3(s) &= (\det m)s^2 + (m_{11}\beta_{22} - m_{12}\beta_{12})s + m_{11}\omega_{22} \\
&\quad - m_{12}\omega_{12}, \\
\mathrm{F}_4(s) &= (m_{12}\beta_{22} - m_{22}\beta_{12})s + m_{12}\omega_{22} - m_{22}\omega_{12}, \\
\mathrm{F}_5(s) &= m_{22}s^2 + \beta_{22}s + \omega_{22}, \\
\mathrm{F}_6(s) &= -m_{12}s^2 - \beta_{12}s - \omega_{12},
\end{aligned}$$

where $\det m = m_{11}m_{12} - m_{12}^2$ and $\det\beta = \beta_{11}\beta_{22} - \beta_{12}^2$.

The time-dependent factors in the expression of $\langle x_2(t)\rangle$ in Eq. (11) read $C_j(t) = \mathrm{L}^{-1}[\mathrm{F}_{j+2}(s)/\mathrm{P}(s)]$ $(j = 5, \ldots, 8)$ from the inverse Laplace transforms, where

$$\begin{aligned}
\mathrm{F}_7(s) &= (m_{12}\omega_{11} - m_{11}\omega_{12})s + \beta_{12}\omega_{11} - \beta_{11}\omega_{12}, \\
\mathrm{F}_8(s) &= (\det m)s^3 + (m_{11}\beta_{22} + m_{22}\beta_{11} - 2m_{12}\beta_{12})s^2 \\
&\quad + (m_{22}\omega_{11} - m_{12}\omega_{12} + \det\beta)s + \beta_{22}\omega_{11} \\
&\quad - \beta_{12}\omega_{12}, \\
\mathrm{F}_9(s) &= (m_{12}\beta_{11} - m_{11}\beta_{12})s + m_{12}\omega_{11} - m_{11}\omega_{12}, \\
\mathrm{F}_{10}(s) &= (\det m)s^2 + (m_{22}\beta_{11} - m_{12}\beta_{12})s + m_{22}\omega_{11} \\
&\quad - m_{12}\omega_{12}. \qquad \text{(A2)}
\end{aligned}$$

[1] H. Hofmann and R. Samhammer, Z. Phys. A **322**, 157 (1985).
[2] Y. Aritomo, T. Wada, M. Ohta, and Y. Abe, Phys. Rev. C **55**, R1011 (1997); **59**, 796 (1999); Y. Abe, Y. Aritomo, T. Wada, and M. Ohta, J. Phys. G **23**, 1275 (1997).
[3] W. J. Świątecki, K. Siwek-Wilczyńska, and J. Wilczyński, Phys. Rev. C **71**, 014602 (2005).
[4] C. E. Aguiar, V. C. Barbosa, R. Donangelo, and S. R. Souza, Nucl. Phys. **A491**, 301 (1989).
[5] C. E. Aguiar, V. C. Barbosa, and R. Donangelo, Nucl. Phys. **A517**, 205 (1990).
[6] Y. Abe, D. Boilley, B. G. Giraud, and T. Wada, Phys. Rev. E **61**, 1125 (2000).
[7] J. D. Bao and D. Boilley, Nucl. Phys. **A707**, 47 (2002).
[8] N. Takigawa, S. Ayik, K. Washiyama, and S. Kimura, Phys. Rev. C **69**, 054605 (2004).
[9] S. Ayik, B. Yilmaz, A. Gokalp, O. Yilmaz, and N. Takigawa, Phys. Rev. C **71**, 054611 (2005).

[10] D. Boilley, Y. Abe, and J. D. Bao, Eur. Phys. J. A **18**, 627 (2003).
[11] J. D. Bao and Y. Z. Zhuo, Phys. Rev. C **67**, 064606 (2003).
[12] C. R. Morton, A. C. Berriman, R. D. Butt, M. Dasgupta, D. J. Hinde, A. Godley, J. O. Newton, and K. Hagino, Phys. Rev. C **64**, 034604 (2001).
[13] I. I. Gontchar, M. Dasgupta, D. J. Hinde, R. D. Butt, and A. Mukherjee, Phys. Rev. C **65**, 034610 (2002).
[14] I. I. Gontchar, D. J. Hinde, M. Dasgupta, C. R. Morton, and J. O. Newton, Phys. Rev. C **73**, 034610 (2006).
[15] J.-S. Zhang and H. A. Weidenmüller, Phys. Rev. C **28**, 2190 (1983).
[16] K.-H. Schmidt and W. Morawek, Rep. Prog. Phys. **54**, 949 (1991).
[17] M. Brack, J. Damgaard, A. S. Jensen, H. C. Pauli, V. M. Strutinsky, and C. Y. Wong, Rev. Mod. Phys. **44**, 320 (1972).
[18] Y. Jia and J. D. Bao, Phys. Rev. C **75**, 034601 (2007).